

Non-integer-spin bosonic excitations in untextured magnets

Akashdeep Kamra,^{1,*} Utkarsh Agrawal,² and Wolfgang Belzig^{1,†}

¹*Department of Physics, University of Konstanz, D-78457 Konstanz, Germany*

²*Department of Physics, Indian Institute of Technology Bombay, Powai, Mumbai-400076, India*

Interactions are responsible for intriguing physics, e.g. emergence of exotic ground states and excitations, in a wide range of systems. Here we theoretically demonstrate that dipole-dipole interaction leads to bosonic eigen-excitations with spin ranging from zero to above \hbar in magnets with uniformly magnetized ground states. These exotic excitations can be interpreted as quantum coherent conglomerates of magnons, the eigen-excitations when the dipolar interactions are disregarded. We further find that the eigenmodes in an easy-axis antiferromagnet are spin-zero quasiparticles instead of the widely believed spin $\pm\hbar$ magnons. The latter re-emerge when the symmetry is broken by a sufficiently large applied magnetic field. The spin greater than \hbar is accompanied by vacuum fluctuations and may be considered a weak form of frustration.

PACS numbers: 75.45.+j, 75.10.-b, 75.30.Ds

Introduction. Interactions among the entities constituting a physical system determine its qualitative behavior. Even a simple metal, typically described as a free (non-interacting) electron gas, comprises an electronic Fermi liquid [1] with the quasiparticle effective mass subtly absorbing the interaction effects. These quasiparticles however maintain same charge (e) and spin ($\hbar/2$) as that of a single electron. Relatively exotic states are exemplified by the superconducting phase, in which phonon-mediated electron-electron interaction leads to the formation of Cooper pairs with charge $2e$, and the fractional quantum hall phase [2] composed of fractional-charge quasiparticles [3–5].

In a ferromagnet (FM), the exchange interaction favors a spin-aligned ground state. Considering only Zeeman and exchange interactions, the eigen-excitations are charge-neutral, spin \hbar bosonic quasiparticles - magnons [6], where the role of exchange is again absorbed in the magnon effective mass. Magnetic dipolar interaction (DI) between these otherwise “non-interacting” magnons lead to formation of new quasiparticles - squeezed magnons [7]. Furthermore, dipolar and spin-orbit interactions often result in textured ground states, such as domain walls [8] and skyrmions [9, 10], exhibiting rich physics.

Analogously, antiferromagnets [11] (AFs) admit the so-called Neel-ordered ground state with two interpenetrating, equivalent, and anti-collinear sublattices resulting in a vanishing net magnetization. The magnetic order without any associated magnetization and stray fields has led to a strong interest in employing AFs for spintronic applications [12, 13] with demonstrated success [14]. The normal excitations in AFs are believed to be similar in nature to the magnons in FMs [6], with the former kind’s much larger energies being dominated by the inter-sublattice antiferromagnetic exchange. Typically, this large energy argument is employed to justify disregarding DI in considering AF magnons [12, 15–18]. While there is some merit to the energy comparison, inso-

far as accounting for DI leaves the AF magnon energies essentially unchanged, the concomitant breaking of the rotational invariance of the spin system leads to qualitatively important and novel effects that form a part of the results reported herein.

Apart from the ordered configurations discussed above, magnets also allow phases, called spin liquids [19, 20], with long-range spin correlations without any static spin-order. This intriguing phenomenon, called geometrical frustration, may occur when each spin faces conflicting demands from its neighbors as to the direction in which the spin should point, for example in a triangular lattice AF. A static spin-order is absent in such a system because it fluctuates between a multitude of degenerate states with opposite net spins. Spin-liquids are believed to host several exotic excitations [19, 20] such as magnetic monopoles [21], spinons [22–24], triplons etc. and are speculated as a possible precursor to high- T_C superconductivity [25, 26]. While nearest-neighbor exchange models are often employed to capture the essential physics, the DI plays an important role in some spin-liquids, for instance in spin-ice systems [27, 28], in which magnetic monopoles have recently been observed [29, 30].

In this Letter, we theoretically investigate excitations in magnets with homogeneous spin-ordered ground states laying special emphasis on the role of DI. The easy-axis two-sublattice model employed herein encompasses the full range from FMs via ferrimagnets to AFs. Our key finding is that DI relaxes the spin conservation constraint and results in exotic bosonic quasiparticles with non-integral spin ranging from zero to greater than \hbar (Fig. 1). These new quasiparticles can be physically understood as quantum coherent conglomerates of spin $\pm\hbar$ magnons, where spin-nonconserving coherence is mediated by DI. Specifically, we find that quasiparticles in AFs with equivalent sublattices possess zero spin and are non-degenerate [Fig. 1 (c)], in contrast with the wide belief based upon theories that disregard DI [12, 15–18]. These quasiparticles continuously approach spin

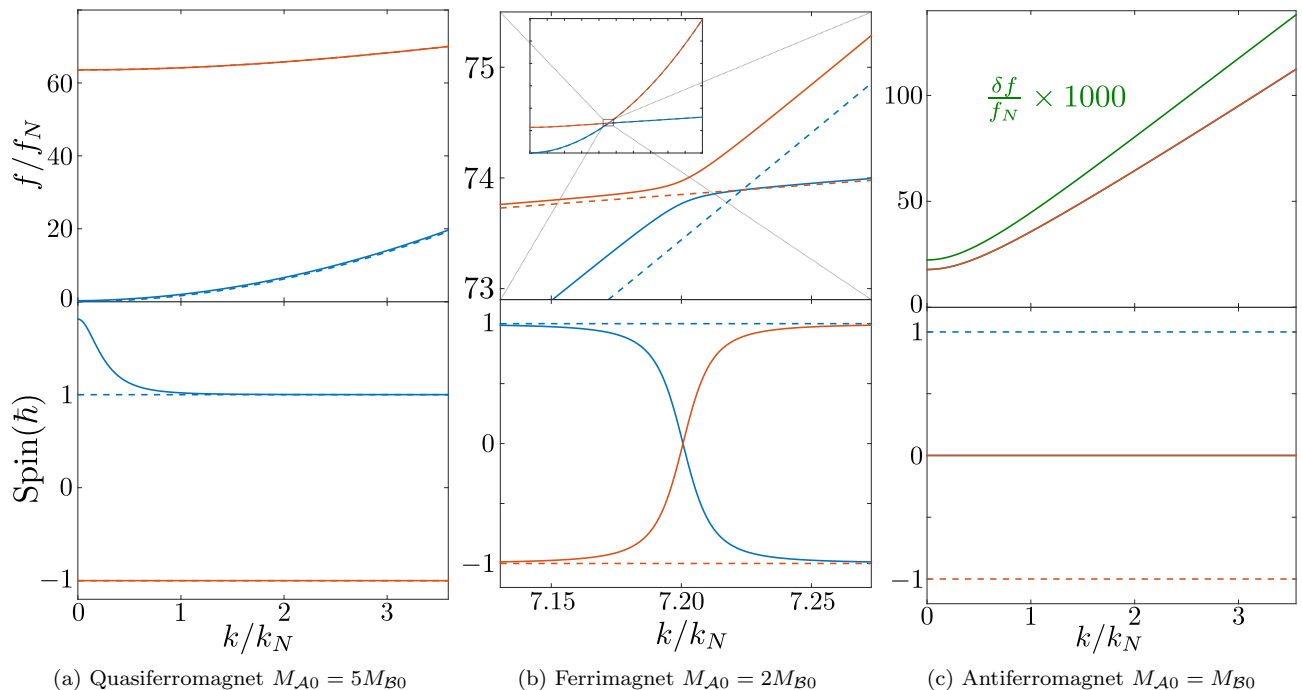


FIG. 1. Dispersion along x-direction (upper panels) and quasiparticle spin (lower panels) for three kinds of magnets. Solid and dashed lines respectively denote the results with and without DI. $2\pi f_N = |\gamma_A|\mu_0 M_{A0}$ and $f_i(k_N) = 2 \times \max[f_N, f_i(0)]$ define the normalizations f_N , k_N with $f_i(k)$ the lower dispersion band. (a) The low energy band mimics magnon dispersion in a ferromagnet. Quasiparticles at low (comparable to dipolar) energies exhibit squeezing and spin greater than \hbar [7]. (b) Region around the dispersion anticrossing point is shown with the upper panel inset depicting the full dispersion. Quasiparticles with spin varying between $+\hbar$ and $-\hbar$ are formed around the anticrossing point. (c) Degeneracy of the two bands in antiferromagnets is lifted by DI with splitting δf in the GHz range. Quasiparticle spin in both bands vanishes.

$\pm\hbar$ magnons, due to broken sublattice equivalence, as the applied magnetic field becomes much larger than the sublattice saturation magnetization (Fig. 2). The squeezing-mediated [7] quasiparticle spin greater than \hbar is inevitably accompanied by vacuum fluctuations which decrease the net spin in the ground state. We argue that this behavior is also a consequence of large ground state degeneracy, and is thus a weak, non-geometrical form of frustration that only diminishes the ground state net spin.

Theoretical model. We start by outlining the method. The first step is formulating the classical free energy density of two antiferromagnetically coupled sublattices \mathcal{A} and \mathcal{B} in terms of their respective magnetizations $\mathbf{M}_{\mathcal{A},\mathcal{B}}(\mathbf{r})$ [31]. With ferromagnetic intrasublattice exchange and easy-axis anisotropy along z-direction, the ground state is Neel ordered, i.e. $\mathbf{M}_{\mathcal{A},\mathcal{B}}(\mathbf{r}) = \pm M_{A0,B0}\hat{z} + \delta\mathbf{M}_{\mathcal{A},\mathcal{B}}(\mathbf{r})$. Here $M_{A0,B0}$ are the respective sublattice saturation magnetizations, and $\delta\mathbf{M}_{\mathcal{A},\mathcal{B}}(\mathbf{r})$ describe the excitations with $|\delta\mathbf{M}_{\mathcal{A},\mathcal{B}}(\mathbf{r})| \ll M_{A0,B0}$. The quantum Hamiltonian density is then obtained by replacing classical $[\mathbf{M}_{\mathcal{A},\mathcal{B}}(\mathbf{r})]$ with quantum [32] field variables $\tilde{\mathbf{M}}_{\mathcal{A},\mathcal{B}}(\mathbf{r})$ [6, 31]. The Holstein-Primakoff trans-

formations [6, 31, 33] substitute $\tilde{\mathbf{M}}_{\mathcal{A},\mathcal{B}}(\mathbf{r})$ in terms of the bosonic ladder operators $\tilde{a}(\mathbf{r}), \tilde{b}(\mathbf{r}')$ that, respectively, represent annihilation operators of a magnon on the sublattices \mathcal{A}, \mathcal{B} at positions \mathbf{r}, \mathbf{r}' . Integrating the ensuing Hamiltonian density over the entire volume yields the system Hamiltonian in terms of the Fourier space magnon operators $\tilde{a}_{\mathbf{k}}, \tilde{b}_{\mathbf{k}'}$. Finally, the eigen-excitations and the corresponding dispersion are obtained by diagonalizing the Hamiltonian using a four-dimensional Bogoliubov transform.

The classical free energy density for the two-sublattice system described above comprises of Zeeman (H_Z), magnetocrystalline anisotropy (H_{an}), exchange (H_{ex}), and dipolar (H_{dip}) interaction terms. With an applied magnetic field $H_0\hat{z}$ and μ_0 the permeability of free space, the Zeeman energy density reads $H_Z = -\mu_0 H_0 (M_{Az} + M_{Bz})$. The easy-axis anisotropy is parametrized in terms of the constants K_{uA}, K_{uB} as $H_{an} = -K_{uA}M_{Az}^2 - K_{uB}M_{Bz}^2$ [31]. In a minimalistic model, the exchange energy density is expressed in terms of the constants $\mathcal{J}_A, \mathcal{J}_B, \mathcal{J}_{AB}$ and \mathcal{J} as follows [31]: $H_{ex} = \sum_{x_i=x,y,z} [\mathcal{J}_A(\partial\mathbf{M}_A/\partial x_i) \cdot (\partial\mathbf{M}_A/\partial x_i) + \mathcal{J}_B(\partial\mathbf{M}_B/\partial x_i) \cdot (\partial\mathbf{M}_B/\partial x_i) + \mathcal{J}_{AB}(\partial\mathbf{M}_A/\partial x_i) \cdot (\partial\mathbf{M}_B/\partial x_i)] + \mathcal{J}\mathbf{M}_A \cdot \mathbf{M}_B$. The DI energy density is obtained in terms of the demag-

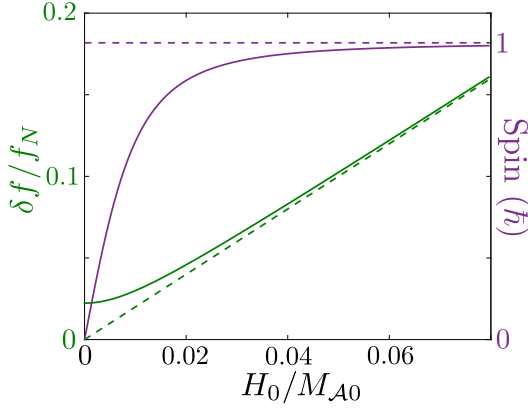


FIG. 2. Normalized band splitting ($2\pi f_N = |\gamma_A|\mu_0 M_{A0}$) and quasiparticle spin vs. applied magnetic field (H_0) in easy-axis antiferromagnets. Solid and dashed lines respectively denote the results with and without DI.

netization field \mathbf{H}_m [6, 31]: $H_{\text{dip}} = -(1/2)\mu_0\mathbf{H}_m \cdot (\mathbf{M}_A + \mathbf{M}_B)$. The demagnetization field is related to the magnetization via the Maxwell's equations simplified within the magnetostatic approximation [6, 31, 34].

In order to quantize the Hamiltonian, we recognize the relation between magnetization and spin density operators: $\tilde{\mathbf{M}}_{A,B}(\mathbf{r}) = -|\gamma_{A,B}|\tilde{\mathbf{S}}_{A,B}(\mathbf{r})$, where $\gamma_{A,B}$ are the respective gyromagnetic ratios assumed to be negative here. The commutation relations for the magnetization components can be obtained using spin commutation rules, and are satisfied by the Holstein-Primakoff transformations [33] generalized to the two sub-lattice model [6, 16]. To the lowest order, the latter are given by: $\tilde{M}_{A+}(\mathbf{r}) = \sqrt{2|\gamma_A|\hbar M_{A0}} \tilde{a}(\mathbf{r})$, $\tilde{M}_{B+}(\mathbf{r}) = \sqrt{2|\gamma_B|\hbar M_{B0}} \tilde{b}(\mathbf{r})$, $\tilde{M}_{Az}(\mathbf{r}) = M_{A0} - \hbar|\gamma_A|\tilde{a}^\dagger(\mathbf{r})\tilde{a}(\mathbf{r})$, and $\tilde{M}_{Bz}(\mathbf{r}) = -M_{B0} + \hbar|\gamma_B|\tilde{b}^\dagger(\mathbf{r})\tilde{b}(\mathbf{r})$. Here, $\tilde{M}_{A+} = \tilde{M}_{A-}^\dagger = \tilde{M}_{Ax} + i(\gamma_A/|\gamma_A|)\tilde{M}_{Ay}$, and similar for the sublattice B . The final step in obtaining the Hamiltonian is integrating the energy density operator over the volume.

Delegating details to the supplemental material [34], the Hamiltonian is thus obtained in terms of the k-space magnon ladder operators $\tilde{a}_{\mathbf{k}}, \tilde{b}_{\mathbf{k}}$:

$$\tilde{\mathcal{H}} = \sum_{\mathbf{k}} \left[\frac{A_{\mathbf{k}}}{2} \tilde{a}_{\mathbf{k}}^\dagger \tilde{a}_{\mathbf{k}} + \frac{B_{\mathbf{k}}}{2} \tilde{b}_{\mathbf{k}}^\dagger \tilde{b}_{\mathbf{k}} + C_{\mathbf{k}} \tilde{a}_{\mathbf{k}} \tilde{b}_{-\mathbf{k}} + D_{\mathbf{k}} \tilde{a}_{\mathbf{k}} \tilde{a}_{-\mathbf{k}} + E_{\mathbf{k}} \tilde{b}_{\mathbf{k}} \tilde{b}_{-\mathbf{k}} + F_{\mathbf{k}} \tilde{a}_{\mathbf{k}} \tilde{b}_{\mathbf{k}}^\dagger \right] + \text{h.c.} \quad (1)$$

Analytical expressions for the coefficients $A_{\mathbf{k}}, B_{\mathbf{k}} \dots$ are given in the supplemental material [34]. Here, we simply note some of their properties: $A_{\mathbf{k}}, B_{\mathbf{k}}$ are real and positive, $C_{\mathbf{k}}$ are real, and $D_{\mathbf{k}}, E_{\mathbf{k}}, F_{\mathbf{k}}$ are, in general, complex. All the coefficients stay unchanged on replacing \mathbf{k} with $-\mathbf{k}$. We also note that the terms with $D_{\mathbf{k}}, E_{\mathbf{k}}, F_{\mathbf{k}}$ are entirely due to DI, and do not conserve the system spin.

In order to diagonalize the Hamiltonian, it is conve-

nient to define a new wavevector index $\boldsymbol{\kappa}$ that runs over only half of the wavevector space [33]. We define a four-dimensional Bogoliubov transform to new bosonic operators $\tilde{\alpha}_{\pm\boldsymbol{\kappa}}, \tilde{\beta}_{\pm\boldsymbol{\kappa}}$:

$$\begin{pmatrix} \tilde{\alpha}_{\boldsymbol{\kappa}} \\ \tilde{\beta}_{-\boldsymbol{\kappa}}^\dagger \\ \tilde{\alpha}_{-\boldsymbol{\kappa}}^\dagger \\ \tilde{\beta}_{\boldsymbol{\kappa}} \end{pmatrix} = \begin{pmatrix} u_1 & v_1 & w_1 & x_1 \\ u_2 & v_2 & w_2 & x_2 \\ u_3 & v_3 & w_3 & x_3 \\ u_4 & v_4 & w_4 & x_4 \end{pmatrix} \begin{pmatrix} \tilde{a}_{\boldsymbol{\kappa}} \\ \tilde{b}_{-\boldsymbol{\kappa}}^\dagger \\ \tilde{a}_{-\boldsymbol{\kappa}}^\dagger \\ \tilde{b}_{\boldsymbol{\kappa}} \end{pmatrix} = \underline{S} \begin{pmatrix} \tilde{a}_{\boldsymbol{\kappa}} \\ \tilde{b}_{-\boldsymbol{\kappa}}^\dagger \\ \tilde{a}_{-\boldsymbol{\kappa}}^\dagger \\ \tilde{b}_{\boldsymbol{\kappa}} \end{pmatrix}, \quad (2)$$

with the requirement that it diagonalizes the Hamiltonian to $\tilde{\mathcal{H}} = \sum_{\boldsymbol{\kappa}} [\epsilon_{\alpha\boldsymbol{\kappa}}(\tilde{\alpha}_{\boldsymbol{\kappa}}^\dagger \tilde{\alpha}_{\boldsymbol{\kappa}} + \tilde{\alpha}_{-\boldsymbol{\kappa}}^\dagger \tilde{\alpha}_{-\boldsymbol{\kappa}}) + \epsilon_{\beta\boldsymbol{\kappa}}(\tilde{\beta}_{\boldsymbol{\kappa}}^\dagger \tilde{\beta}_{\boldsymbol{\kappa}} + \tilde{\beta}_{-\boldsymbol{\kappa}}^\dagger \tilde{\beta}_{-\boldsymbol{\kappa}})]$. The subscript $\boldsymbol{\kappa}$ of \underline{S} and its elements has been suppressed for brevity. Since $A_{\boldsymbol{\kappa}}, B_{\boldsymbol{\kappa}} \dots$ are invariant with respect to the replacement $\boldsymbol{\kappa} \rightarrow -\boldsymbol{\kappa}$, the same is true for $\epsilon_{\alpha\boldsymbol{\kappa}}, \epsilon_{\beta\boldsymbol{\kappa}}$ and \underline{S} . This invariance also leads to the relations $S_{22} = S_{11}^*$ and $S_{21} = S_{12}^*$, where S_{ij} are 2×2 matrix blocks that constitute \underline{S} . Bosonic commutation rules for $\tilde{\alpha}_{\pm\boldsymbol{\kappa}}, \tilde{\beta}_{\pm\boldsymbol{\kappa}}, \tilde{a}_{\pm\boldsymbol{\kappa}}, \tilde{b}_{\pm\boldsymbol{\kappa}}$ further impose relations on \underline{S} elements, all of which can be succinctly expressed as:

$$\underline{S} \underline{Y} \underline{S}^\dagger = \underline{Y} \implies \underline{S}^{-1} = \underline{Y} \underline{S}^\dagger \underline{Y}^{-1}, \quad (3)$$

where $\underline{Y} = \sigma_z \otimes \sigma_z$, with σ_z the third Pauli matrix. Employing the diagonal form of $\tilde{\mathcal{H}}$, we obtain $[\tilde{\alpha}_{\boldsymbol{\kappa}}, \tilde{\mathcal{H}}] = \epsilon_{\alpha\boldsymbol{\kappa}} \tilde{\alpha}_{\boldsymbol{\kappa}}$, from which Eqs. (1) and (2) lead to the eigenvalue problem $\underline{T}_{\boldsymbol{\kappa}} \xi_{1\boldsymbol{\kappa}} = \epsilon_{\alpha\boldsymbol{\kappa}} \xi_{1\boldsymbol{\kappa}}$ with

$$\underline{T}_{\boldsymbol{\kappa}} = \begin{pmatrix} A_{\boldsymbol{\kappa}} & -C_{\boldsymbol{\kappa}} & -2D_{\boldsymbol{\kappa}} & F_{\boldsymbol{\kappa}} \\ C_{\boldsymbol{\kappa}} & -B_{\boldsymbol{\kappa}} & -F_{\boldsymbol{\kappa}} & 2E_{\boldsymbol{\kappa}}^* \\ 2D_{\boldsymbol{\kappa}}^* & -F_{\boldsymbol{\kappa}}^* & -A_{\boldsymbol{\kappa}} & C_{\boldsymbol{\kappa}} \\ F_{\boldsymbol{\kappa}}^* & -2E_{\boldsymbol{\kappa}} & -C_{\boldsymbol{\kappa}} & B_{\boldsymbol{\kappa}} \end{pmatrix}, \quad \xi_{1\boldsymbol{\kappa}} = \begin{pmatrix} u_1 \\ v_1 \\ w_1 \\ x_1 \end{pmatrix}. \quad (4)$$

Employing $[\tilde{\beta}_{\boldsymbol{\kappa}}, \tilde{\mathcal{H}}] = \epsilon_{\beta\boldsymbol{\kappa}} \tilde{\beta}_{\boldsymbol{\kappa}}$ in an analogous way yields a similar eigenvalue problem $\underline{T}_{\boldsymbol{\kappa}} \xi_{4\boldsymbol{\kappa}} = \epsilon_{\beta\boldsymbol{\kappa}} \xi_{4\boldsymbol{\kappa}}$. The multiplicative constants for eigenvectors are fixed by Eq. (3). Since $S_{22} = S_{11}^*$, $S_{21} = S_{12}^*$, knowledge of $\xi_{1\boldsymbol{\kappa}}, \xi_{4\boldsymbol{\kappa}}$ provides the complete transformation matrix \underline{S} .

While the eigenvalue problem at hand is analytically solvable, we do not present the unwieldy solution here. Instead, we provide the dispersion and eigenvectors *disregarding* DI:

$$\epsilon'_{\alpha\boldsymbol{\kappa}, \beta\boldsymbol{\kappa}} = \frac{\pm(A'_{\boldsymbol{\kappa}} - B'_{\boldsymbol{\kappa}}) + \sqrt{(A'_{\boldsymbol{\kappa}} + B'_{\boldsymbol{\kappa}})^2 - 4(C'_{\boldsymbol{\kappa}})^2}}{2}, \quad \xi'_{1\boldsymbol{\kappa}} = [qn_4, n_2, 0, 0]^T; \quad \xi'_{4\boldsymbol{\kappa}} = [0, 0, qn_2, n_4]^T, \quad (5)$$

where $q = C'_{\boldsymbol{\kappa}}/|C'_{\boldsymbol{\kappa}}|$, $n_{2,4} = (1/\sqrt{2})\sqrt{1/\sqrt{1-\delta^2} \mp 1}$, and $\delta = 2C'_{\boldsymbol{\kappa}}/(A'_{\boldsymbol{\kappa}} + B'_{\boldsymbol{\kappa}})$. Here, the primed notation emphasizes that all the coefficients have been evaluated *disregarding* DI.

Excitation spectrum and properties. We are primarily interested in the eigen-excitation spin. With the total volume \mathcal{V} , z-component of the total spin $\tilde{\mathbf{S}}(\mathbf{r}) = \tilde{\mathbf{S}}_A(\mathbf{r}) + \tilde{\mathbf{S}}_B(\mathbf{r})$ is evaluated using the employed Holstein-

Primakoff and Bogoliubov [Eq. (2)] transformations:

$$\int_{\mathcal{V}} d^3r \langle \tilde{S}_z(\mathbf{r}) \rangle = - \left[\frac{M_{\mathcal{A}0}\mathcal{V}}{|\gamma_{\mathcal{A}0}|} - \frac{M_{\mathcal{B}0}\mathcal{V}}{|\gamma_{\mathcal{B}0}|} \right] + \hbar \sum_{\kappa} T_{2\kappa} + \hbar \sum_{\kappa} T_{3\kappa}, \quad (6)$$

where $T_{2\kappa} = |w_1|^2 - |v_1|^2 + |u_2|^2 - |x_2|^2 + |u_3|^2 - |x_3|^2 + |w_4|^2 - |v_4|^2$ and $T_{3\kappa} = \{(1 + 2(|w_1|^2 - |x_1|^2))n_{\alpha\kappa} - \{(1 + 2(|x_2|^2 - |w_2|^2))n_{\beta-\kappa} + \{(1 + 2(|u_3|^2 - |v_3|^2))n_{\alpha-\kappa} - \{(1 + 2(|v_4|^2 - |u_4|^2))n_{\beta\kappa}$. In Eq. (6) above, the first term denotes the total spin of a fully saturated Neel-ordered state, while the second expresses vacuum fluctuations. The third term represents the contribution of the quasiparticles with n_X the number of \tilde{X} quasiparticles, and the curly bracketed prefactor of n_X denoting the corresponding quasiparticle spin (in units of \hbar).

We consider three cases - quasiferromagnet, ferrimagnet, and antiferromagnet - that exhibit, disregarding DI, 0, 1 and infinite crossing points on the dispersion diagram. From Eqs. (5) and (6), we note that the quasiparticle spin in all these cases remains $\pm\hbar$ if DI is disregarded. Together, these three cases encompass all topologically distinct dispersions allowed in our system. Since our model is applicable over a broad domain, we refrain from assigning parameters values corresponding to a particular material, and simply affirm to typical orders of magnitude for the different parameters [12]. Deferring the specification of the exact values to supplemental material [34], we choose intrasublattice exchange, intersublattice exchange, easy-axis anisotropy, and sublattice saturation magnetization around 1000 T, 100 T, 0.1 T, and 100 kA/m [12], respectively. We further assume the magnetic specimen to be a film in the y-z plane.

By quasiferromagnet, we refer to a system with one sublattice dominating over the other [Fig. 1(a)]. As a result, one dispersion branch is much lower in energy than the other and behaves like in a ferromagnet. A prototypical example of such a material is yttrium iron garnet [35, 36]. Figure 1(a) shows that the quasiparticles in a part of this low energy band have spin greater than \hbar . This is due to the DI-mediated squeezing of magnons as predicted in ferromagnets [7]. The high-energy band does not change considerably due to DI since the latter is much weaker than the antiferromagnetic exchange, which dominates this band.

When both sublattices have comparable properties, for example in gadolinium iron garnet [37], the two bands may (anti)cross as shown in Fig.1(b). Two primary effects of DI can be seen in the dispersion: (i) the crossing is converted into an anticrossing, and (ii) the corresponding wavevector is shifted owing to the DI contribution to the band energies. Around this anticrossing point [$k \approx \sqrt{\mathcal{J}(|\gamma_{\mathcal{A}}|M_{\mathcal{A}0} - |\gamma_{\mathcal{B}}|M_{\mathcal{B}0})}/2(\mathcal{J}_{\mathcal{A}}|\gamma_{\mathcal{A}}|M_{\mathcal{A}0} - \mathcal{J}_{\mathcal{B}}|\gamma_{\mathcal{B}}|M_{\mathcal{B}0})$], the two kinds of magnons hybridize creating new quasiparticles with spin varying continuously between $\pm\hbar$.

We further note that the quasiparticle spin in the low wavenumber region, not depicted in Fig. 1(b), is greater than \hbar due to squeezing.

Antiferromagnets have sublattices with identical properties resulting in, disregarding DI, two degenerate bands. This degeneracy is spontaneously lifted, with the band splitting δf in the GHz range, by DI [Fig. 1(c)]. The resulting quasiparticles are superpositions of spin $\pm\hbar$ magnons, and possess zero spin. The band degeneracy can also be lifted by a magnetic field applied along the anisotropy axis which breaks the symmetry between the two sublattices. When this field is much larger than the sublattice saturation magnetizations, the effects of DI can be disregarded as shown in Fig. 2.

Discussion. While the quasiparticles discussed above have several exotic properties, the emphasis here has been on their non-integral spin. This is partly because their spin is amenable to experimental observation [7, 38]. Current shot noise [39], i.e. the fluctuations in a (charge, spin etc.) current due to its flow in discrete lumps carried by the quasiparticles, has proven to be a robust probe into the quantum of transport. It has already been shown that spin current shot noise in a magnet|non-magnetic conductor bilayer may provide experimental access to the quasiparticle spin [7, 38].

Equation (6) indicates that non-integral spin and vacuum fluctuations are two facets of the same phenomenon. In particular, we know that squeezing [7, 40] simultaneously leads to quasiparticle spin larger than \hbar and vacuum fluctuations. Here we discuss suggestive similarities between squeezed ground state and complex frustrated spin-ice systems [28]. Much like in the latter [19], the essential ingredient to squeezing of the ground state is DI, and not antiferromagnetic exchange. Physically, DI allows pairs of magnons to be spontaneously created or destroyed in the system [see Eq. (1)]. In other words, squeezed magnons are superpositions of magnon number states differing by multiples of two, possessing a large degeneracy. The large degeneracy of the ground state is also considered a defining feature of frustration [19]. While squeezing merely reduces the net spin in the ground state, geometrical frustration completely annihilates it. However, squeezing is not dependent upon the system geometry and hence constitutes a different kind of frustration.

Summary. We predict exotic bosonic quasiparticles with non-integral spin in magnets with simple uniformly magnetized ground states. The formation of these quasiparticles requires relaxation of spin conservation in the system, which in our case is provided by the magnetic dipolar interaction. In particular, we find that easy-axis antiferromagnets can host spin-zero quasiparticles. The qualitatively new insights gained into the nature of quasiparticles in antiferromagnets fills an important gap in our understanding of these systems, which have recently found their niche in applications [13, 14]. We also suggest a connection between spontaneous squeezing and

“non-geometrical” frustration which might motivate use of quantum optics knowledge in understanding complex solid state systems.

Acknowledgments. We acknowledge financial support from the Alexander von Humboldt Foundation and the DFG through SFB 767. UA thanks the Belzig group members for their kind hospitality during his visit to Konstanz.

* akashdeep.kamra@uni-konstanz.de

† wolfgang.belzig@uni-konstanz.de

- [1] G. E. Brown, “Landau, brueckner-bethe, and migdal theories of fermi systems,” *Rev. Mod. Phys.* **43**, 1–14 (1971).
- [2] R. B. Laughlin, “Anomalous quantum hall effect: An incompressible quantum fluid with fractionally charged excitations,” *Phys. Rev. Lett.* **50**, 1395–1398 (1983).
- [3] J. K. Jain, “Composite-fermion approach for the fractional quantum hall effect,” *Phys. Rev. Lett.* **63**, 199–202 (1989).
- [4] L. Saminadayar, D. C. Glattli, Y. Jin, and B. Etienne, “Observation of the $e/3$ fractionally charged laughlin quasiparticle,” *Phys. Rev. Lett.* **79**, 2526–2529 (1997).
- [5] M. Reznikov, R. de Picciotto, T. G. Griffiths, M. Heiblum, and V. Umansky, “Observation of quasiparticles with one-fifth of an electron’s charge,” *Nature* **399**, 238 (1999).
- [6] C. Kittel, *Quantum theory of solids* (Wiley, New York, 1963).
- [7] Akashdeep Kamra and Wolfgang Belzig, “Superpoissonian shot noise of squeezed-magnon mediated spin transport,” *Phys. Rev. Lett.* **116**, 146601 (2016).
- [8] Charles Kittel, “Physical theory of ferromagnetic domains,” *Rev. Mod. Phys.* **21**, 541–583 (1949).
- [9] A. N. Bogdanov and U. K. Röbner, “Chiral symmetry breaking in magnetic thin films and multilayers,” *Phys. Rev. Lett.* **87**, 037203 (2001).
- [10] Roland Wiesendanger, “Nanoscale magnetic skyrmions in metallic films and multilayers: a new twist for spintronics,” *Nature Reviews Materials* **1**, 16044 (2016).
- [11] Strictly speaking, we consider easy-axis AFs in which the spins prefer to align along a certain direction.
- [12] E. V. Gomonay and V. M. Loktev, “Spintronics of antiferromagnetic systems (review article),” *Low Temperature Physics* **40**, 17–35 (2014).
- [13] T. Jungwirth, X. Marti, P. Wadley, and J. Wunderlich, “Antiferromagnetic spintronics,” *Nature Nanotechnology* **11**, 231 (2016).
- [14] P. Wadley, B. Howells, J. Železný, C. Andrews, V. Hills, R. P. Campion, V. Novák, K. Olejník, F. Maccherozzi, S. S. Dhesi, S. Y. Martin, T. Wagner, J. Wunderlich, F. Freimuth, Y. Mokrousov, J. Kuneš, J. S. Chauhan, M. J. Grzybowski, A. W. Rushforth, K. W. Edmonds, B. L. Gallagher, and T. Jungwirth, “Electrical switching of an antiferromagnet,” *Science* **351**, 587–590 (2016).
- [15] F. Keffer and C. Kittel, “Theory of antiferromagnetic resonance,” *Phys. Rev.* **85**, 329–337 (1952).
- [16] Yuichi Ohnuma, Hiroto Adachi, Eiji Saitoh, and Sadamichi Maekawa, “Spin seebeck effect in antiferromagnets and compensated ferrimagnets,” *Phys. Rev. B* **87**, 014423 (2013).
- [17] Ran Cheng, Jiang Xiao, Qian Niu, and Arne Brataas, “Spin pumping and spin-transfer torques in antiferromagnets,” *Phys. Rev. Lett.* **113**, 057601 (2014).
- [18] S. M. Rezende, R. L. Rodríguez-Suárez, and A. Azevedo, “Theory of the spin seebeck effect in antiferromagnets,” *Phys. Rev. B* **93**, 014425 (2016).
- [19] Leon Balents, “Spin liquids in frustrated magnets,” *Nature* **464**, 199 (2010).
- [20] L. Savary and L. Balents, “Quantum Spin Liquids,” *ArXiv e-prints* (2016), arXiv:1601.03742 [cond-mat.str-el].
- [21] C. Castelnovo, R. Moessner, and S. L. Sondhi, “Spin liquids in frustrated magnets,” *Nature* **451**, 42 (2008).
- [22] Ian Affleck and J. Brad Marston, “Large- n limit of the heisenberg-hubbard model: Implications for high- T_c superconductors,” *Phys. Rev. B* **37**, 3774–3777 (1988).
- [23] N. Read and Subir Sachdev, “Large- N expansion for frustrated quantum antiferromagnets,” *Phys. Rev. Lett.* **66**, 1773–1776 (1991).
- [24] Walter Rantner and Xiao-Gang Wen, “Electron spectral function and algebraic spin liquid for the normal state of underdoped high T_c superconductors,” *Phys. Rev. Lett.* **86**, 3871–3874 (2001).
- [25] P. W. Anderson, “The resonating valence bond state in la_2cuo_4 and superconductivity,” *Science* **235**, 1196–1198 (1987).
- [26] Patrick A. Lee, Naoto Nagaosa, and Xiao-Gang Wen, “Doping a mott insulator: Physics of high-temperature superconductivity,” *Rev. Mod. Phys.* **78**, 17–85 (2006).
- [27] M. J. Harris, S. T. Bramwell, D. F. McMorrow, T. Zeiske, and K. W. Godfrey, “Geometrical frustration in the ferromagnetic pyrochlore $ho_2ti_2O_7$,” *Phys. Rev. Lett.* **79**, 2554–2557 (1997).
- [28] Steven T. Bramwell and Michel J. P. Gingras, “Spin ice state in frustrated magnetic pyrochlore materials,” *Science* **294**, 1495–1501 (2001).
- [29] D. J. P. Morris, D. A. Tennant, S. A. Grigera, B. Klemke, C. Castelnovo, R. Moessner, C. Czternasty, M. Meissner, K. C. Rule, J.-U. Hoffmann, K. Kiefer, S. Gerischer, D. Slobinsky, and R. S. Perry, “Dirac strings and magnetic monopoles in the spin ice $dy_2ti_2o_7$,” *Science* **326**, 411–414 (2009).
- [30] Hiroaki Kadowaki, Naohiro Doi, Yuji Aoki, Yoshikazu Tabata, Taku J. Sato, Jeffrey W. Lynn, Kazuyuki Matsuhira, and Zenji Hiroi, “Observation of magnetic monopoles in spin ice,” *Journal of the Physical Society of Japan* **78**, 103706 (2009).
- [31] A.I. Akhiezer, V.G. Bar’iakhhtar, and S.V. Peletminski, *Spin waves* (North-Holland Publishing Company, Amsterdam, 1968).
- [32] Here, and in the rest of the manuscript, we employ tilde to represent quantum operators.
- [33] T. Holstein and H. Primakoff, “Field dependence of the intrinsic domain magnetization of a ferromagnet,” *Phys. Rev.* **58**, 1098–1113 (1940).
- [34] See supplemental material for details on the derivation of the Hamiltonian and values of the various parameters used in the plots.
- [35] Mathias Weiler, Matthias Althammer, Michael Schreier, Johannes Lotze, Matthias Pernpeintner, Sibylle Meyer, Hans Huebl, Rudolf Gross, Akashdeep Kamra, Jiang Xiao, Yan-Ting Chen, HuJun Jiao, Gerrit E. W. Bauer, and Sebastian T. B. Goennenwein, “Experimental test

- of the spin mixing interface conductivity concept,” Phys. Rev. Lett. **111**, 176601 (2013).
- [36] Joseph Barker and Gerrit E. W. Bauer, “Thermal spin dynamics of yttrium iron garnet,” Phys. Rev. Lett. **117**, 217201 (2016).
- [37] Stephan Geprägs, Andreas Kehlberger, Francesco Della Coletta, Zhiyong Qiu, Er-Jia Guo, Tomek Schulz, Christian Mix, Sibylle Meyer, Akashdeep Kamra, Matthias Althammer, Hans Huebl, Gerhard Jakob, Yuichi Ohnuma, Hiroto Adachi, Joseph Barker, Sadamichi Maekawa, Gerrit E. W. Bauer, Eiji Saitoh, Rudolf Gross, Sebastian T. B. Goennenwein, and Mathias Kläui, “Origin of the spin seebeck effect in compensated ferrimagnets,” Nature Communications **7**, 10452 (2016).
- [38] Akashdeep Kamra and Wolfgang Belzig, “Magnon-mediated spin current noise in ferromagnet | nonmagnetic conductor hybrids,” Phys. Rev. B **94**, 014419 (2016).
- [39] Ya.M. Blanter and M. Büttiker, “Shot noise in mesoscopic conductors,” Physics Reports **336**, 1 – 166 (2000).
- [40] D.F. Walls and G.J. Milburn, *Quantum Optics* (Springer, Berlin, 2008).
-

Supplementary material with the manuscript Non-integer-spin bosonic excitations in untextured magnets by

Akashdeep Kamra, Utkarsh Agrawal and Wolfgang Belzig

DERIVATION OF THE HAMILTONIAN

The classical Hamiltonian for the system is given by the integral of energy density over the entire volume \mathcal{V} :

$$\mathcal{H} = \int_{\mathcal{V}} d^3r (H_Z + H_{\text{an}} + H_{\text{ex}} + H_{\text{dip}}), \quad (\text{S1})$$

$$= \mathcal{H}_Z + \mathcal{H}_{\text{an}} + \mathcal{H}_{\text{ex}} + \mathcal{H}_{\text{dip}}, \quad (\text{S2})$$

with contributions from Zeeman, anisotropy, exchange and dipolar interaction energies. With an applied magnetic field $H_0 \hat{\mathbf{z}}$, the Zeeman contribution reads:

$$\mathcal{H}_Z = - \int_{\mathcal{V}} d^3r \mu_0 H_0 (M_{\mathcal{A}z} + M_{\mathcal{B}z}), \quad (\text{S3})$$

where $\mathbf{M}_{\mathcal{A}}, \mathbf{M}_{\mathcal{B}}$ are the magnetization fields corresponding to the two sublattices. Quantization of Hamiltonian is achieved by replacing the classical variables $\mathbf{M}_{\mathcal{A}}, \mathbf{M}_{\mathcal{B}}$ with the corresponding quantum operators $\tilde{\mathbf{M}}_{\mathcal{A}}, \tilde{\mathbf{M}}_{\mathcal{B}}$. The Holstein-Primakoff (HP) transformation [6, 33] given by:

$$\tilde{M}_{\mathcal{A}+}(\mathbf{r}) = \sqrt{2|\gamma_{\mathcal{A}}|\hbar M_{\mathcal{A}0}} \tilde{a}(\mathbf{r}), \quad (\text{S4})$$

$$\tilde{M}_{\mathcal{B}+}(\mathbf{r}) = \sqrt{2|\gamma_{\mathcal{B}}|\hbar M_{\mathcal{B}0}} \tilde{b}^\dagger(\mathbf{r}), \quad (\text{S5})$$

$$\tilde{M}_{\mathcal{A}z}(\mathbf{r}) = M_{\mathcal{A}0} - \hbar|\gamma_{\mathcal{A}}|\tilde{a}^\dagger(\mathbf{r})\tilde{a}(\mathbf{r}), \quad (\text{S6})$$

$$\tilde{M}_{\mathcal{B}z}(\mathbf{r}) = -M_{\mathcal{B}0} + \hbar|\gamma_{\mathcal{B}}|\tilde{b}^\dagger(\mathbf{r})\tilde{b}(\mathbf{r}), \quad (\text{S7})$$

expresses the magnetization in terms of the magnonic ladder operators $\tilde{a}(\mathbf{r}), \tilde{b}(\mathbf{r})$ corresponding, respectively, to the two sublattices \mathcal{A}, \mathcal{B} . In the above transformation, $\tilde{M}_{P+} = \tilde{M}_{P-}^\dagger = \tilde{M}_{Px} + (\gamma_P/|\gamma_P|)i\tilde{M}_{Py}$, and γ_P, M_{P0} are the gyromagnetic ratio and the saturation magnetization corresponding to sublattice P. Employing HP transformation [Eqs. (S4) - (S7)] into Eq. (S3), we obtain the Zeeman contribution to the Hamilton operator:

$$\tilde{\mathcal{H}}_Z = \sum_{\mathbf{k}} \mu_0 H_0 \hbar (|\gamma_{\mathcal{A}}|\tilde{a}_{\mathbf{k}}^\dagger \tilde{a}_{\mathbf{k}} - |\gamma_{\mathcal{B}}|\tilde{b}_{\mathbf{k}}^\dagger \tilde{b}_{\mathbf{k}}), \quad (\text{S8})$$

where $\tilde{a}_{\mathbf{k}}, \tilde{b}_{\mathbf{k}}$ are the magnon operators in the k-space, and we have dropped the constant contribution to the Hamiltonian.

Proceeding along analogous lines, we now consider the easy-axis anisotropy energy:

$$\mathcal{H}_{\text{an}} = \int_{\mathcal{V}} d^3r (-K_{\text{u}\mathcal{A}}M_{\mathcal{A}z}^2 - K_{\text{u}\mathcal{B}}M_{\mathcal{B}z}^2), \quad (\text{S9})$$

where $K_{\text{u}\mathcal{A}}, K_{\text{u}\mathcal{B}}$ parametrize the energy density [31]. On quantization and HP transformation, we obtain the corresponding contribution to the Hamiltonian as:

$$\tilde{\mathcal{H}}_{\text{an}} = \hbar \sum_{\mathbf{k}} 2K_{\text{u}\mathcal{A}}|\gamma_{\mathcal{A}}|M_{\mathcal{A}0}\tilde{a}_{\mathbf{k}}^\dagger \tilde{a}_{\mathbf{k}} + 2K_{\text{u}\mathcal{B}}|\gamma_{\mathcal{B}}|M_{\mathcal{B}0}\tilde{b}_{\mathbf{k}}^\dagger \tilde{b}_{\mathbf{k}}. \quad (\text{S10})$$

The analogous classical and quantum Hamiltonians corresponding to the exchange energy are [31]:

$$\mathcal{H}_{\text{ex}} = \int_{\mathcal{V}} d^3r \left[\sum_{x_i=x,y,z} \left\{ \mathcal{J}_{\mathcal{A}} \frac{\partial \mathbf{M}_{\mathcal{A}}}{\partial x_i} \cdot \frac{\partial \mathbf{M}_{\mathcal{A}}}{\partial x_i} + \mathcal{J}_{\mathcal{B}} \frac{\partial \mathbf{M}_{\mathcal{B}}}{\partial x_i} \cdot \frac{\partial \mathbf{M}_{\mathcal{B}}}{\partial x_i} + \mathcal{J}_{\mathcal{AB}} \frac{\partial \mathbf{M}_{\mathcal{A}}}{\partial x_i} \cdot \frac{\partial \mathbf{M}_{\mathcal{B}}}{\partial x_i} \right\} + \mathcal{J} \mathbf{M}_{\mathcal{A}} \cdot \mathbf{M}_{\mathcal{B}} \right], \quad (\text{S11})$$

$$\begin{aligned} \tilde{\mathcal{H}}_{\text{ex}} = & \hbar \sum_{\mathbf{k}} \left[2\mathcal{J}_{\mathcal{A}} k^2 |\gamma_{\mathcal{A}}| M_{\mathcal{A}0} + \mathcal{J} |\gamma_{\mathcal{B}}| M_{\mathcal{B}0} \right] \tilde{a}_{\mathbf{k}}^{\dagger} \tilde{a}_{\mathbf{k}} \\ & + \hbar \sum_{\mathbf{k}} \left[2\mathcal{J}_{\mathcal{B}} k^2 |\gamma_{\mathcal{B}}| M_{\mathcal{B}0} + \mathcal{J} |\gamma_{\mathcal{A}}| M_{\mathcal{A}0} \right] \tilde{b}_{\mathbf{k}}^{\dagger} \tilde{b}_{\mathbf{k}} \\ & + \hbar \sum_{\mathbf{k}} \left[\mathcal{J}_{\mathcal{AB}} k^2 \sqrt{|\gamma_{\mathcal{A}}| M_{\mathcal{A}0} |\gamma_{\mathcal{B}}| M_{\mathcal{B}0}} + \mathcal{J} \sqrt{|\gamma_{\mathcal{A}}| M_{\mathcal{A}0} |\gamma_{\mathcal{B}}| M_{\mathcal{B}0}} \right] \left(\tilde{a}_{\mathbf{k}} \tilde{b}_{-\mathbf{k}} + \tilde{a}_{\mathbf{k}}^{\dagger} \tilde{b}_{-\mathbf{k}}^{\dagger} \right), \end{aligned} \quad (\text{S12})$$

where $\mathcal{J}_{\mathcal{A}}$, $\mathcal{J}_{\mathcal{B}}$ parametrize the intrasublattice exchange while $\mathcal{J}_{\mathcal{AB}}$, \mathcal{J} parametrize intersublattice exchange interaction.

The dipolar interaction is treated within a mean field approximation via the so-called demagnetization field \mathbf{H}_m generated by the magnetization:

$$\mathcal{H}_{\text{dip}} = - \int_{\mathcal{V}} d^3r \frac{1}{2} \mu_0 \mathbf{H}_m \cdot \mathbf{M}, \quad (\text{S13})$$

with $\mathbf{M} = \mathbf{M}_{\mathcal{A}0} + \mathbf{M}_{\mathcal{B}0}$ the total magnetization. The magnetization and the demagnetization field are split into spatially uniform and non-uniform contributions $\mathbf{H}_m = \mathbf{H}_u + \mathbf{H}_{nu}$ and $\mathbf{M} = \mathbf{M}_u + \mathbf{M}_{nu}$ thereby affording the following relation between the uniform components [6, 31]:

$$\mathbf{H}_u = -N_x M_{ux} \hat{\mathbf{x}} - N_y M_{uy} \hat{\mathbf{y}} - N_z M_{uz} \hat{\mathbf{z}}, \quad (\text{S14})$$

where $N_{x,y,z}$ are the eigenvalues of the demagnetization tensor which is diagonal in the chosen coordinate system. Within the magnetostatic approximation, the non-uniform components obey the equations [6, 31]:

$$\nabla \times \mathbf{H}_{nu} = 0, \quad (\text{S15})$$

$$\nabla \cdot (\mathbf{H}_{nu} + \mathbf{M}_{nu}) = 0. \quad (\text{S16})$$

Employing the equations above and HP transformation [Eqs. (S4) - (S7)], straightforward albeit lengthy algebra leads to the following expression for the dipolar contribution to the Hamiltonian:

$$\begin{aligned} \tilde{\mathcal{H}}_{\text{dip}} = & \hbar \mu_0 |\gamma_{\mathcal{A}}| \sum_{\mathbf{k}} \left[N_z (M_{\mathcal{B}0} - M_{\mathcal{A}0}) + \delta_{\mathbf{k},\mathbf{0}} \frac{N_x + N_y}{2} M_{\mathcal{A}0} + (1 - \delta_{\mathbf{k},\mathbf{0}}) \frac{\sin^2(\theta_{\mathbf{k}})}{2} M_{\mathcal{A}0} \right] \tilde{a}_{\mathbf{k}}^{\dagger} \tilde{a}_{\mathbf{k}} \\ & + \hbar \mu_0 |\gamma_{\mathcal{B}}| \sum_{\mathbf{k}} \left[N_z (M_{\mathcal{A}0} - M_{\mathcal{B}0}) + \delta_{\mathbf{k},\mathbf{0}} \frac{N_x + N_y}{2} M_{\mathcal{B}0} + (1 - \delta_{\mathbf{k},\mathbf{0}}) \frac{\sin^2(\theta_{\mathbf{k}})}{2} M_{\mathcal{B}0} \right] \tilde{b}_{\mathbf{k}}^{\dagger} \tilde{b}_{\mathbf{k}} \\ & + \hbar \mu_0 \sqrt{|\gamma_{\mathcal{A}}| M_{\mathcal{A}0} |\gamma_{\mathcal{B}}| M_{\mathcal{B}0}} \sum_{\mathbf{k}} \left[\delta_{\mathbf{k},\mathbf{0}} \frac{N_x + N_y}{2} + (1 - \delta_{\mathbf{k},\mathbf{0}}) \frac{\sin^2(\theta_{\mathbf{k}})}{2} \right] \left(\tilde{a}_{\mathbf{k}} \tilde{b}_{-\mathbf{k}} + \tilde{a}_{\mathbf{k}}^{\dagger} \tilde{b}_{-\mathbf{k}}^{\dagger} \right) \\ & + \left\{ \hbar \mu_0 |\gamma_{\mathcal{A}}| M_{\mathcal{A}0} \sum_{\mathbf{k}} \left[\delta_{\mathbf{k},\mathbf{0}} \frac{N_x - N_y}{4} + (1 - \delta_{\mathbf{k},\mathbf{0}}) \frac{\sin^2(\theta_{\mathbf{k}})}{4} e^{i2\phi_{\mathbf{k}}} \right] \tilde{a}_{\mathbf{k}} \tilde{a}_{-\mathbf{k}} \right\} + \text{h.c.} \\ & + \left\{ \hbar \mu_0 |\gamma_{\mathcal{B}}| M_{\mathcal{B}0} \sum_{\mathbf{k}} \left[\delta_{\mathbf{k},\mathbf{0}} \frac{N_x - N_y}{4} + (1 - \delta_{\mathbf{k},\mathbf{0}}) \frac{\sin^2(\theta_{\mathbf{k}})}{4} e^{-i2\phi_{\mathbf{k}}} \right] \tilde{b}_{\mathbf{k}} \tilde{b}_{-\mathbf{k}} \right\} + \text{h.c.} \\ & + \left\{ \hbar \mu_0 \sqrt{|\gamma_{\mathcal{A}}| M_{\mathcal{A}0} |\gamma_{\mathcal{B}}| M_{\mathcal{B}0}} \sum_{\mathbf{k}} \left[\delta_{\mathbf{k},\mathbf{0}} \frac{N_x - N_y}{2} + (1 - \delta_{\mathbf{k},\mathbf{0}}) \frac{\sin^2(\theta_{\mathbf{k}})}{2} e^{i2\phi_{\mathbf{k}}} \right] \tilde{a}_{\mathbf{k}} \tilde{b}_{\mathbf{k}}^{\dagger} \right\} + \text{h.c.} \quad , \end{aligned} \quad (\text{S17})$$

where $\theta_{\mathbf{k}}$ and $\phi_{\mathbf{k}}$ are the polar and azimuthal angles of \mathbf{k} .

Combining Eqs. (S8), (S10), (S12) and (S17), the full Hamiltonian reads:

$$\tilde{\mathcal{H}} = \sum_{\mathbf{k}} \left[\frac{A_{\mathbf{k}}}{2} \tilde{a}_{\mathbf{k}}^{\dagger} \tilde{a}_{\mathbf{k}} + \frac{B_{\mathbf{k}}}{2} \tilde{b}_{\mathbf{k}}^{\dagger} \tilde{b}_{\mathbf{k}} + C_{\mathbf{k}} \tilde{a}_{\mathbf{k}} \tilde{b}_{-\mathbf{k}} + D_{\mathbf{k}} \tilde{a}_{\mathbf{k}} \tilde{a}_{-\mathbf{k}} + E_{\mathbf{k}} \tilde{b}_{\mathbf{k}} \tilde{b}_{-\mathbf{k}} + F_{\mathbf{k}} \tilde{a}_{\mathbf{k}} \tilde{b}_{\mathbf{k}}^{\dagger} \right] + \text{h.c.} \quad , \quad (\text{S18})$$

where

$$\begin{aligned} \frac{A_{\mathbf{k}}}{\hbar} = & \mu_0 H_0 |\gamma_{\mathcal{A}}| + 2K_{u\mathcal{A}} |\gamma_{\mathcal{A}}| M_{\mathcal{A}0} + 2\mathcal{J}_{\mathcal{A}} k^2 |\gamma_{\mathcal{A}}| M_{\mathcal{A}0} + \mathcal{J} |\gamma_{\mathcal{B}}| M_{\mathcal{B}0} \\ & + \mu_0 |\gamma_{\mathcal{A}}| \left[N_z (M_{\mathcal{B}0} - M_{\mathcal{A}0}) + \delta_{\mathbf{k},\mathbf{0}} \frac{N_x + N_y}{2} M_{\mathcal{A}0} + (1 - \delta_{\mathbf{k},\mathbf{0}}) \frac{\sin^2(\theta_{\mathbf{k}})}{2} M_{\mathcal{A}0} \right], \end{aligned} \quad (\text{S19})$$

$$\begin{aligned} \frac{B_{\mathbf{k}}}{\hbar} = & -\mu_0 H_0 |\gamma_{\mathcal{B}}| + 2K_{u\mathcal{B}} |\gamma_{\mathcal{B}}| M_{\mathcal{B}0} + 2\mathcal{J}_{\mathcal{B}} k^2 |\gamma_{\mathcal{B}}| M_{\mathcal{B}0} + \mathcal{J} |\gamma_{\mathcal{A}}| M_{\mathcal{A}0} \\ & + \mu_0 |\gamma_{\mathcal{B}}| \left[N_z (M_{\mathcal{A}0} - M_{\mathcal{B}0}) + \delta_{\mathbf{k},\mathbf{0}} \frac{N_x + N_y}{2} M_{\mathcal{B}0} + (1 - \delta_{\mathbf{k},\mathbf{0}}) \frac{\sin^2(\theta_{\mathbf{k}})}{2} M_{\mathcal{B}0} \right], \end{aligned} \quad (\text{S20})$$

$$\frac{C_{\mathbf{k}}}{\hbar} = \sqrt{|\gamma_{\mathcal{A}}| M_{\mathcal{A}0} |\gamma_{\mathcal{B}}| M_{\mathcal{B}0}} \left[\mathcal{J} + \mathcal{J}_{\mathcal{AB}} k^2 + \mu_0 \delta_{\mathbf{k},\mathbf{0}} \frac{N_x + N_y}{2} + \mu_0 (1 - \delta_{\mathbf{k},\mathbf{0}}) \frac{\sin^2(\theta_{\mathbf{k}})}{2} \right], \quad (\text{S21})$$

$$\frac{D_{\mathbf{k}}}{\hbar} = \mu_0 |\gamma_{\mathcal{A}}| M_{\mathcal{A}0} \left[\delta_{\mathbf{k},\mathbf{0}} \frac{N_x - N_y}{4} + (1 - \delta_{\mathbf{k},\mathbf{0}}) \frac{\sin^2(\theta_{\mathbf{k}})}{4} e^{i2\phi_{\mathbf{k}}} \right], \quad (\text{S22})$$

$$\frac{E_{\mathbf{k}}}{\hbar} = \mu_0 |\gamma_{\mathcal{B}}| M_{\mathcal{B}0} \left[\delta_{\mathbf{k},\mathbf{0}} \frac{N_x - N_y}{4} + (1 - \delta_{\mathbf{k},\mathbf{0}}) \frac{\sin^2(\theta_{\mathbf{k}})}{4} e^{-i2\phi_{\mathbf{k}}} \right], \quad (\text{S23})$$

$$F_{\mathbf{k}} = 2\sqrt{D_{\mathbf{k}} E_{\mathbf{k}}^*}. \quad (\text{S24})$$

VALUES OF MODEL PARAMETERS

Parameter	Quasiferromagnet	Ferrimagnet	Antiferromagnet	Units
$\mu_0 H_0$	0.05	0.05	0	T
N_x, N_y, N_z	1,0,0	1,0,0	1,0,0	Dimensionless
$\gamma_{\mathcal{A}}$	1.8	1.8	1.8	$\times 10^{11} \text{ s}^{-1} \text{ T}^{-1}$
$\gamma_{\mathcal{B}}$	1.8	1.8	1.8	$\times 10^{11} \text{ s}^{-1} \text{ T}^{-1}$
$M_{\mathcal{A}}$	5	5	5	$\times 10^5 \text{ A/m}$
$M_{\mathcal{B}}$	1	2.5	5	$\times 10^5 \text{ A/m}$
$\mathcal{J}_{\mathcal{A}}$	1	5	1	$\times 10^{-23} \text{ J} \cdot \text{mA}^{-2}$
$\mathcal{J}_{\mathcal{B}}$	1	1	1	$\times 10^{-23} \text{ J} \cdot \text{mA}^{-2}$
$\mathcal{J}_{\mathcal{AB}}$	0.1	0.1	0.1	$\times 10^{-23} \text{ J} \cdot \text{mA}^{-2}$
\mathcal{J}	1	1	5	$\times 10^{-4} \text{ Jm}^{-1} \text{ A}^{-2}$
$K_{u\mathcal{A}}$	2	2	2	$\times 10^{-7} \text{ Jm}^{-1} \text{ A}^{-2}$
$K_{u\mathcal{B}}$	2	2	2	$\times 10^{-7} \text{ Jm}^{-1} \text{ A}^{-2}$